

†Work supported by the U. S. Atomic Energy Commission under Contract No. AT(30-1)-1238.

¹G. van Hoven, *Phys. Rev. Lett.* **17**, 169 (1966); H. Derfler and T. C. Simonen, *Phys. Rev. Lett.* **17**, 172 (1966).

²J. H. Malmberg and C. B. Wharton, *Phys. Rev. Lett.* **13**, 184 (1964), and **17**, 175 (1966).

³Y. Nakamura and M. Ito, *Phys. Rev. Lett.* **26**, 350 (1971).

⁴S. C. Brown, *Basic Data of Plasma Physics* (Mass-

achusetts Institute of Technology Press, Cambridge, Mass., 1959).

⁵H. H. Kuehl, G. E. Stewart, and C. Yeh, *Phys. Fluids* **8**, 723 (1965).

⁶J. W. S. Rayleigh, *The Theory of Sound* (Dover, New York, 1945), 2nd ed.

⁷J. L. Bogdanov and J. E. Wellett, *J. Appl. Phys.* **41**, 2601 (1970).

⁸K. Nishikawa, private communication.

Direct Optical Coupling to Surface Excitations

A. S. Barker, Jr.

Bell Telephone Laboratories, Murray Hill, New Jersey 07974

(Received 7 February 1972)

A method is described of directly coupling an optical beam to surface excitations. Using this technique the frequency and linewidth of surface plasmons in doped germanium and in gold and surface phonons in calcium molybdate are determined. The method also allows the dispersion curve to be measured.

Surface plasmons are wave-type excitations which can exist at the surface of a metal or doped semiconductor.^{1,2} These excitations were first detected by electron scattering from thin metal foils.³ Similar surface phonon excitations have been detected by slow-electron reflection spectroscopy.⁴ Recently an indirect optical beam interaction has been reported for the case where the surface is roughened either in a random manner⁵ or by ruling a grating.⁶ Theoretical attempts to fit such optical experiments are considerably hampered by the complications introduced by the roughness itself.⁷ The present paper shows a very direct method of coupling to surface modes of plasmon, phonon, exciton, or mixed character. The surface remains undisturbed and the method allows the coupling to be calculated exactly.

A surface plasmon or surface phonon wave is characterized by an electric field which oscillates in time and varies sinusoidally in directions along the surface but falls off exponentially in the directions perpendicular to the surface. Figure 1 shows the spatial pattern of the electric field. In the figure, k is the wave vector along the surface. The actual form of the electric field for large k is

$$\vec{E} = E_0(\hat{x} + i\hat{z})e^{i(kx - \omega t)}e^{-k|z|}, \quad (1)$$

where \hat{x} and \hat{z} are unit vectors as shown in the Fig. 1(a). The dispersion curve for surface plasmons is illustrated in Fig. 1(b).⁸ For k large compared to ω/c but still very much smaller

than k_F ,⁹ the dispersion curve becomes horizontal and is asymptotic to the frequency determined by

$$\text{Re}[\epsilon(\omega)] = -1. \quad (2)$$

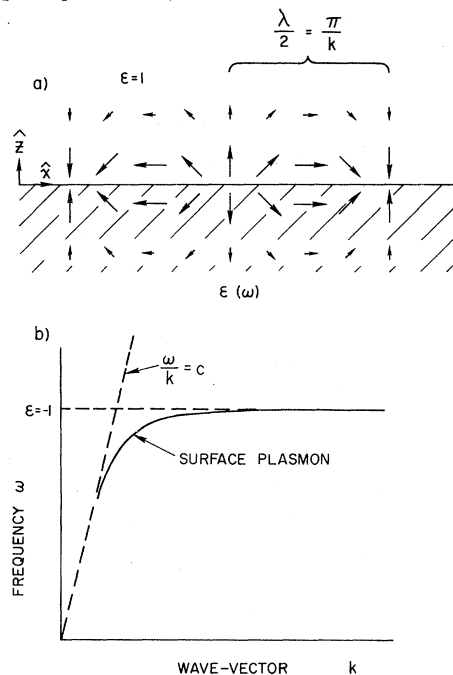


FIG. 1. (a) Spatial dependence of the electric vector for a surface plasmon or phonon. The wave propagates along the x direction and has maximum amplitude at the interface between the two media. (b) Surface plasmon dispersion curve for an air-metal interface. For an air-dielectric interface, the small- k part of the curve can drop only as far as the frequency where ϵ has its pole.

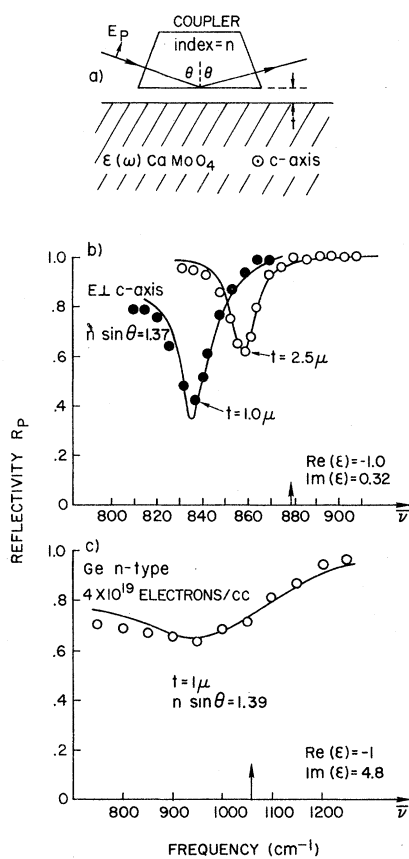


FIG. 2. (a) Coupling device of index n placed a small distance above the surface of the medium whose surface mode is to be studied. A p -polarized light beam is reflected from the lower surface of the coupler. (b) The reflectivity R_p for CaMoO_4 displaying a surface-phonon dip. (c) R_p for Ge showing a broad surface-plasmon dip. In both materials $\epsilon(\omega)$ is measured separately using normal-incidence reflectivity without the coupler. The solid curves are calculated from Fresnel's equations for the geometry shown using the measured $\epsilon(\omega)$ and the known index and angle in the coupler.

Equation (2) holds for a vacuum-metal interface, where $\epsilon(\omega)$ is the dielectric constant of the metal.^{2,10}

Figure 2(a) shows a p -polarized optical beam undergoing total internal reflection at a dielectric-air interface. The electric field pattern on the air side of the interface is called an evanescent wave, and it has exactly the form given by Eq. (1) with wave vector along the surface given by

$$k_1 = n\omega \sin(\theta)/c. \tag{3}$$

Here n is the index of refraction of the dielectric, ω is the frequency of the optical beam, and c the velocity of light. From the similarity of the elec-

tric field pattern of the evanescent wave and that of the surface plasmon of Fig. 1, we might expect coupling of the two when the two surfaces are brought within a distance $t \sim 1/k_1$ of each other. In this situation the beam in the dielectric does not undergo total reflection because some of the energy is used to excite the surface plasmon. Hence one should observe a reflection dip at the frequency of the surface plasmon whose wave vector k_1 matches k_1 of Eq. (3). Since k_1 can be varied by our choice of n and θ , the dispersion of the surface excitation may be probed. All of the above considerations hold for a medium which has sufficient dispersion for $\epsilon(\omega)$ to pass through the value -1 . It is immaterial whether the dispersion is connected with plasmons, optical phonons, excitons, or mixtures of these.

Figure 2(b) shows the experimentally measured reflectivity of a CaMoO_4 surface as detected using a coupling prism of BaF_2 ($n = 1.39$ at 850 cm^{-1}). A prominent dip is seen just below the frequency¹¹ where $\text{Re}(\epsilon) = -1$. The spacing between the prism and the CaMoO_4 surface was controlled by evaporating metal dots to act as spacers. Figure 2(b) shows the effect of changing the coupling by changing t . As the coupling is reduced (t increased) the surface phonon dip approaches the frequency 864 cm^{-1} and linewidth 12 cm^{-1} . For a driving frequency of 864 cm^{-1} , the wave vector k_1 is 7442 cm^{-1} . At this small wave vector the dispersion of the surface phonon is rather evident, the dip falling 14 cm^{-1} below the frequency where $\text{Re}(\epsilon) = -1$. Figure 2(c) shows the effect of surface-plasmon creation in doped Ge. Here the plasmon is quite highly damped by the impurity scattering introduced by the high doping levels. In both experiments no dip is observed for the s -polarized reflectivity, i.e., for \vec{E} normal to the plane of Fig. 2(a).

The surface-mode effects discussed above can be calculated from the Fresnel equations¹² for the three-media geometry of coupler-spacer-sample. The unusual feature here is that the angle of refraction is complex and both real and imaginary parts must be retained. We have done these calculations for s - and p -polarized waves incident on the coupler and obtain good agreement with the measured surface-mode dips of Figs. 2(b) and 2(c). We have also measured two of the ordinary-ray surface phonons in quartz and the surface plasmon in gold (Fig. 3) and here also get good agreement with theory.

In general, surface modes may be described by the electric field response to an applied sur-

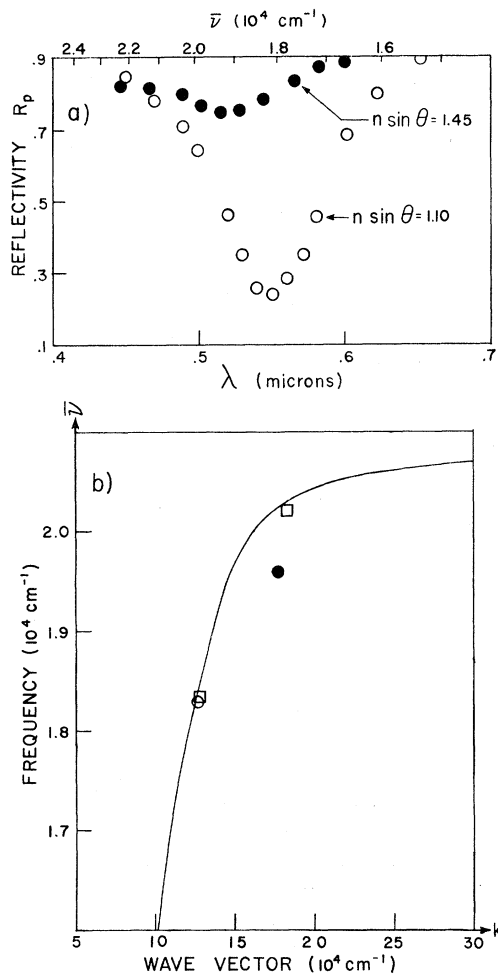


FIG. 3. (a) Measured reflectivity of a thick evaporated gold film using a glass coupler of index $n=1.52$. Two angles of incidence were used as indicated. (b) The two reflectivity minima in (a) give two points on the surface-plasmon dispersion curve plotted as circles. Squares, same data corrected for shifts due to finite coupling. The solid curve is a plot of the peak of $\text{Im}(T)$ using Eq. (4) and the known optical constants of gold.

face charge. This response function contains the resonant factor

$$T = \left[-\epsilon - \frac{(1 - \epsilon\omega^2/c^2k^2)^{1/2}}{(1 - \omega^2/c^2k^2)^{1/2}} \right]^{-1} \quad (4)$$

For large wave vector the expression simplifies to $(-\epsilon - 1)^{-1}$ so that the response function $\text{Im}(T)$ is peaked at the frequency given by Eq. (2). We wish to emphasize that once the complex dielectric function $\epsilon(\omega)$ is known, the frequency, linewidth, and coupling strength of the surface modes may be determined for any wave vector k by examining the poles of T . For example, if the sam-

ple has carriers as well as optical phonons, then ϵ contains phonon and plasma terms and Eq. (4) has two branches of poles, i.e., two surface-wave branches. Thus Eq. (4) can be used to describe the mixed plasmon-phonon surface modes recently observed by Anderson, Alexander, and Bell, on n -type InSb using the surface-grating method.¹³

It is of interest to find the direct relation between the response function T for surface waves and the experimental method described here. In physical terms the evanescent wave allows coupling of a plane-wave beam to a surface excitation via the coupler. Analytically the coupler lets the beam see the surface with an angle of incidence which is complex rather than real. In a *gedanken* experiment let us now remove the coupler but retain the complex angle of incidence. Fresnel's equation for the reflectivity of a single surface is written¹² (for p polarization)

$$r_p = \frac{\sqrt{\epsilon} \cos \theta_1 - \cos \theta_2}{\sqrt{\epsilon} \cos \theta_1 + \cos \theta_2}, \quad (5)$$

where the subscript 1 refers to outside the medium and 2 to inside. We take θ_1 to be complex using Snell's law, $\sin \theta_1 = n \sin \theta$. Using Snell's law again to relate θ_2 to θ_1 we find that the denominator of r_p contains the same resonant terms as the denominator of T .¹⁴ The coupler which causes θ_1 to be complex thus forces the reflectivity response r_p to have the same form as the surface-mode response [Eq. (4)]. We have been able to establish that the reflectivity of the three-media system of Fig. 2 is dominated by this resonance in r_p in the limit of large t (weak coupling). When the coupling is increased, the surface excitation is perturbed and shifted to lower frequency. This result can be understood in the limit of $t \rightarrow 0$ since Eq. (2) becomes $\text{Re}[\epsilon(\omega)] = -n^2$ when the coupler is contiguous with the medium. It can be concluded therefore that the coupler allows excitation of surface modes and direct measurement of their frequency and linewidth. The extensions of the method to Raman scattering by surface modes and to the excitation of surface magnons¹⁵ is straightforward.

Note added in proof.—Otto was apparently the first to propose evanescent wave coupling to surface plasmons¹⁶; however, the extension to other surface excitations has not previously been realized.

The author is indebted to Professor A. J. Sievers, Dr. G. A. Baraff, and Dr. J. M. Rowell for helpful discussions. The capable experimen-

tal help of J. A. Ditzenberger is gratefully acknowledged.

¹R. H. Ritchie, Phys. Rev. 106, 874 (1957).

²E. A. Stern and R. A. Farrell, Phys. Rev. 120, 130 (1960).

³C. J. Powell and J. B. Swan, Phys. Rev. 118, 640 (1960).

⁴H. Ibach, Phys. Rev. Lett. 24, 1416 (1970).

⁵S. E. Schnatterly and S. N. Jasperson, Phys. Rev. 188, 759 (1969).

⁶N. Marschall, B. Fischer, and H. J. Queisser, Phys. Rev. Lett. 27, 95 (1971).

⁷J. Crowell and R. H. Ritchie, J. Opt. Soc. Amer. 60, 794 (1970).

⁸J. M. Elson and R. H. Ritchie, Phys. Rev. B 4, 4129 (1971).

⁹ k_F is the Fermi wave vector. In the case of surface

phonons k must be much less than the reciprocal of the lattice spacing.

¹⁰Strictly speaking Eq. (2) holds only as long as $\text{Im}(\epsilon) = 0$. For finite $\text{Im}(\epsilon)$ the modes are damped with line shapes determined by $\text{Im}[1/(-\epsilon - 1)]$.

¹¹ CaMoO_4 is an insulator with four optical phonons. $\epsilon(\omega)$ passes through -1 four times at four different frequencies. A. S. Barker, Jr., Phys. Rev. 135, A742 (1964).

¹²O. S. Heavens, *Optical Properties of Thin Solid Films* (Academic, New York, 1955), Chap. 4.

¹³W. E. Anderson, R. W. Alexander, Jr., and R. J. Bell, Phys. Rev. Lett. 27, 1057 (1971).

¹⁴M. Cardona, Amer. J. Phys. 39, 1277 (1971), has also noted this behavior of r_p .

¹⁵For the case of antiferromagnetic FeF_2 with its c axis aligned as in Fig. 2, a weak surface-magnon dip should be observable at 53 cm^{-1} for an s -polarized infrared beam in the coupler.

¹⁶A. Otto, Z. Phys. 216, 398 (1968).

Spurious First-Order Phase Transitions in the Self-Consistent Phonon Approximation

E. Pytte

IBM Thomas J. Watson Research Center, Yorktown Heights, New York 10598

(Received 10 December 1971)

It is shown that when the self-consistent phonon approximation is applied to displacive phase transitions, it leads to inconsistent results near the transition point, and that this may give rise to spurious first-order transitions.

Until recently, microscopic theories of displacive phase transitions have been based on a perturbation expansion about a harmonic basis. Since the harmonic soft-mode frequencies are imaginary, the contribution of these modes in the anharmonic terms was neglected. A self-consistent treatment of the soft-mode frequencies was first given by Boccara and Sarma¹ by employing at the onset a renormalized phonon basis. Their formal treatment represented (the lowest order of) what is now called the self-consistent phonon approximation² (SPA). This approximation has been very successful in describing the anharmonic rare-gas solids, including the quantum crystals of solid helium.

Recent numerical calculations have shown that the SPA gives a first-order transition for a model ferroelectric containing only fourth-order anharmonic interactions.³ This result is surprising because the phenomenological Landau (Devonshire) theory predicts the transition to be second order when only terms up to fourth order in the polarization are included.^{4,5} To illustrate the es-

sential features of the SPA and to understand why a first-order transition is obtained, it is instructive to consider a simple model with a single degree of freedom,

$$H = \frac{1}{2} \sum P_l^2 + \frac{1}{2} \Omega_0^2 \sum Q_l^2 - \frac{1}{2} \sum_{ll'} v(ll') Q_l Q_{l'} + \frac{1}{4\gamma} \sum Q_l^4. \quad (1)$$

Here Q_l is a localized normal-mode coordinate describing the ion displacements in cell l , and P_l is the canonical conjugate momentum,

$$[Q_l, P_{l'}] = i\delta_{ll'}. \quad (2)$$

We set $Q_l = Q_0 + u_l$, where the thermal average $Q_0 \equiv \langle Q_l \rangle$ measures the distortion from the high-temperature structure, while u_l describes the fluctuations about the average value. In the SPA the free energy $F = \langle H \rangle - TS$ is obtained by using a harmonic trial density matrix.² The distortion Q_0 and the effective harmonic force constants are determined by minimizing the free energy. For the Hamiltonian given by Eq. (1) the extremum